Localization and Radiation Analysis of Interference Sources Based on UAV Platform

Journal:	*Astronomical Techniques and Instruments*
Manuscript ID	ATI-2025-091.R1
Manuscript Type:	Original Article
Date Submitted by the Author:	21-Mar-2026
Complete List of Authors:	Zhang, Hongrui; Yunnan University, 信息学院; Chinese Academy of Sciences Yunnan Observatory, Dong, Liang; Yunnan Observatories, Chinese Academy of Sciences He, Lesheng ; Yunnan University，, School of Information zhang, ning; 国家无线电监测中心乌鲁木齐监测站 li, shengyang; 云南省无线电监测中心 xi, qiang; Yunnan Observatories, Chinese Academy of Sciences tian, bin; 云南省无线电监测中心 Qin, Yifeng; Yunnan University, 云南大学信息学院 Li, MuDi; Yunnan Observatories, Chinese Academy of Sciences
Keywords:	Unmanned Aerial Vehicle, Interferometric Direction Finding, Signal Source Localization, Electromagnetic Situation, Radiation Analysis
Speciality:	Techniques < Astronomical, Instruments < Astronomical

Astronomical Techniques and Instruments, Vol. 1, January 2026, 560–566

Article Open Access

Localization and Radiation Analysis of Interference Sources Based on UAV Platform

Hongrui Zhang[1], Liang Dong[2]*, Lesheng He[1], Qiang Xi[2], Shengyang Li[3], Bin Tian[3] and Ning Zhang[4]

[1] *School of Information, Yunnan University, Kunming 650500, China;*
[2] *Yunnan Observatories, Chinese Academy of Sciences, Kunming 650011, China;*
[3] *Yunnan Radio Monitoring Center, Kunming 650228, China;*
[4] *Urumqi Monitoring Station of State Radio Monitoring Center, Urumqi, 830011, China.*

*Correspondence: dongliang@ynao.ac.cn
Received: January 27, 2026; Accepted: October 26, 2023; Published Online: December 26, 2023; https://doi.org/10.61977/ati2024999

Citation: Zhang, H.-R. et al. 2026. Localization and Radiation Analysis of Interference Sources Based on UAV Platform , *Astronomical Techniques and Instruments*, **1**(5), 560–566, https://doi.org/10.61977/ati2024999

Abstract: With the widespread use of 5G, low-power, and WiFi wireless devices, radio telescopes are facing increasingly severe interference. These telescopes are usually in areas with complex terrain, making it difficult to accurately locate hidden interference sources using traditional methods and complicating troubleshooting. To address this, this paper proposes an interference source localization and electromagnetic analysis system based on an unmanned aerial vehicle (UAV) platform, aiming to accurately determine the location of interference sources and their radiation distribution in two-dimensional space. The system constructs a spatial multi-baseline switching function based on an airborne circular five-antenna array and a microwave switch matrix. High-precision intersection localization of interference sources is achieved through multi-baseline coherent interferometry, with a localization angle accuracy better than 5 degrees. The digital signal processing part of the system utilizes a zero-intermediate-frequency receiver architecture based on the AD9361, which enables monitoring of signals within the frequency band of 100 MHz to 6 GHz. In terms of electromagnetic situation analysis, the system combines the flight trajectory of the UAV to record signal strength and position information in real-time, and generates an electric field strength distribution map of the interference source in a two-dimensional space. This not only helps to accurately determine the location of the interference source but also effectively assesses the scope of its impact on the radio telescope. Field test verification demonstrates that the system can provide robust data support for interference source identification, localization, and the planning and management of radio protection zones in radio astronomy operations, thereby significantly enhancing the efficiency and accuracy of interference source troubleshooting.

Keywords: Unmanned Aerial Vehicle; Interferometric Direction Finding; Signal Source Localization; Electromagnetic Situation; Radiation Analysis

1. INTRODUCTION

Radio telescopes are important astronomical observation tools that capture radio waves from celestial bodies to study celestial objects such as galaxies, black holes, pulsars, and solar activities, as well as their evolutionary laws. Since radio astronomy operations passively receive radio signals from the universe, the astronomical signals they receive are often extremely weak [1]. With the rapid development of modern communication technologies and the scarcity of radio frequency spectrum resources, radio astronomical observations are facing an increasing number of man-made interferences, which seriously affect the quality and accuracy of observations.

Through research on the localization and troubleshooting of interference sources, the goal is to detect and locate these sources, further eliminate them, identify and reduce such interferences, thereby improving the reliability of observation data and ensuring the normal conduct of radio astronomical observation work.

In recent years, scholars at home and abroad have conducted extensive research on interference source localization methods. In 2021, Zhao Qinghua, Li Jianbin [2], and others proposed a wireless localization algorithm based on TDOA (Time Difference of Arrival) and RSSI (Received Signal Strength Indicator) data fusion. This algorithm optimizes multiple initial position estimates using signal reception strength as weights, improving the localization accuracy by approximately 20%. In 2022, Zhang Haiyan, Hu Hongliang [3], and others proposed an intelligent radio interference monitoring technical solution to meet the demand for high-sensitivity observations of China 's Five-hundred-meter Aperture Spherical radio Telescope (FAST). The core of this solution combines multi-station collaborative spectrum sensing with TDOA-based localization technology to achieve effective identification and accurate localization of interference signals. The adaptive filter in the experiment can effectively suppress interference signals by approximately 30 dB. In 2024, Zhu Kehui, Dong Liang [4], and others proposed a localization algorithm based on joint time-frequency difference analysis to address the interference of high-elevation satellites on radio astronomical observations. Simulation verification showed that the minimum localization error for interference sources at an altitude of 300 kilometers can reach 78 meters.

In terms of improving the accuracy of interference source localization, Li Jun [5] designed a six-channel phase interferometer direction-finding system in 2021. To address the problems of ambiguous azimuth angles and inconsistent amplitude-phase characteristics among channels, he proposed a high-precision direction-finding ambiguity resolution algorithm and a multi-channel amplitude-phase error correction method, and simulation results verified the feasibility of this method for resolving ambiguity. In 2022, Zahra Memarian and Mahdi Majidi [6] proposed a direction-finding method based on a uniform circular array as the reference directional element and an additional central omnidirectional element, building on the coherent interferometer. This method significantly improved the performance and accuracy of Direction of Arrival (DOA) estimation in scenarios involving multiple coherent or non-coherent signal sources and multipath environments. In the same year, Han Jian [7] and others proposed an optimal estimation method for multi-baseline interferometers. Based on the principle of probability theory, this method weights the direction-finding results of different baselines and draws an analogy between this method and the idea of Kalman filtering, verifying its effectiveness. Liu Daorui, Miao Sheng [8] and others addressed the shortcomings of existing detection methods for the quiet zones of the surrounding electromagnetic environment in radio astronomical observations, and proposed a radio interference monitoring method using a four-antenna linear array. In relatively open and quiet environments, this four-antenna array can effectively identify the incoming direction of interference signals, with a reliability of approximately 87% for measurement angle errors not exceeding 5°.

However, in practical scenarios, the terrain around radio telescope sites is relatively complex, mostly in sparsely populated mountainous areas. The obstruction by mountain bodies affects signal propagation [9], which restricts the existing interference source detection and coverage analysis due to the influence of the geographical environment and multipath effects, resulting in poor actual troubleshooting results for interference sources hidden in the terrain. Additionally, handheld monitoring and direction-finding methods consume significant human and time costs.

In recent years, the application scope of UAV (Unmanned Aerial Vehicle) technology has been continuously expanding. Existing studies have applied UAVs to low-altitude electromagnetic environment monitoring to ensure the safe low-altitude operation of general aviation [10]. Introducing UAV technology into spatial electromagnetic detection represents a brand-new approach.

In view of the aforementioned difficulties in troubleshooting radio interference sources at radio telescope sites, the UAV platform provides an efficient solution. In the field of spatial electromagnetic detection, especially in terms of interference source localization and radiation analysis, the application of UAV platforms demonstrates significant advantages, which are specifically reflected in the following aspects:

1. Airborne signal stability: Signals propagating in the air are less affected by multipath effects, making it easier to reduce misjudgments caused by factors such as signal reflection.

2. Minimized impact of terrain factors: For test sites with complex terrain that are difficult to access, UAV platforms can effectively solve the problem of inaccessibility for personnel and vehicles.

3. High-precision intersection localization capability: Relying on the mobility of UAV platforms, rapid interferometric and intersection measurements can be achieved during flight. Therefore, it can perform intersection localization for interference sources hidden in concealed areas such as the interior of buildings and grass.

4. Flexibility in regional radiation analysis: With the 2D spatial movement and position recording function

of UAVs, real-time collection of spatial electromagnetic fields enables the measurement of electromagnetic radiation intensity distribution within the flight area, thereby obtaining information on the spatial distribution of electromagnetic field intensity.

Based on the above background and the advantages of UAV platforms, this paper will introduce the interference source localization and radiation analysis system based on a UAV platform developed by the research team. This system integrates an integrated module for electromagnetic environment monitoring and direction finding on the UAV platform, and uses coherent interferometric direction-finding technology to achieve precise localization of interference sources. The system gives full play to the flexibility and maneuverability of UAVs and combines with an intersection localization strategy to accurately determine the location of interference sources.

In addition, the system also has a spatial radiation collection function. During the UAV's flight, it can record the electromagnetic radiation intensity of the corresponding space along the flight path in real time and draw an electromagnetic situation map, thereby clarifying the radiation impact range of the interference source. This function not only improves the system's ability to monitor and locate interference sources but also provides strong data support for the identification, localization, and management of interference sources.

2. INTRODUCTION TO THE TEST PLATFORM

The primary components of this system include monitoring and direction-finding equipment, a UAV platform, a remote controller, and a monitoring PC terminal, as shown in Figure 1. The monitoring and direction-finding devices consist of an antenna array, a monitoring and direction-finding module, and a digital signal processing board.

The system mainly has the following two functions:

1. Interference Source Direction-Finding: After interference signals are collected by the antenna, the positioning of the interference source is realized through coherent interference direction-finding technology and intersection positioning method.

2. Electromagnetic Situation Analysis: By utilizing the flexibility of the UAV and integrating its geolocation capability, the system tests and stores the interference signal levels within the flight area. It then integrates the flight trajectory to form a spatial electromagnetic situation map, thereby determining the influence range of the interference source.

2.1 Hardware Composition of the System

2.1.1 *Unmanned Aerial Vehicle Platform*

The UAV platform used in the system is the DJI Mavic 3E. This UAV platform has a maximum takeoff weight of 1.05 kg, a maximum ascent and descent speed of 6 m/s, a maximum horizontal flight speed of 15 m/s, and a maximum flight range of 32 km. It features high integration and good stability, which can meet the requirements of most interference source detection tasks. The physical image of the UAV is shown in Figure 2.

The UAV platform consists of two parts: the UAV main body and the onboard payload. Among them, the UAV main body is composed of a power supply module, a detection module, a control unit, and a drive module. Except for the monitoring and direction-finding module in the external mounting, which is developed in this paper, all other components are provided by the DJI Mavic 3E. The overall structure of the UAV platform is shown in Figure 3.

The main composition and function of each part are as follows:

(1) The power supply module consists of three parts: control power supply, external power supply, and power supply. They provide power for the detection module and control unit, external mounting, and drive module, respectively.

(2) The detection module mainly includes an Inertial Measurement Unit (IMU), a barometer, a gyroscope, and a GPS device. It is responsible for realizing the UAV's attitude measurement, altitude detection, and positioning, as well as recording key flight information.

(3) The control module mainly includes a flight control unit, a communication unit, and a data transmission unit. Among them, the flight control unit calculates the current attitude and then generates corresponding control information for the drive module; the communication unit collects the test information of external payloads (cameras and monitoring & direction-finding modules); the data transmission unit transmits the above information to the ground station for observation and storage.

(4) The drive module mainly includes four motors and their drive modules. The power provided is controlled by the control module, which supplies appropriate flight power for the UAV.

2.1.2 *External Payload*

(1) Camera

It is a 4/3-inch CMOS wide-angle camera with 20 million pixels, equipped with a mechanical shutter. It

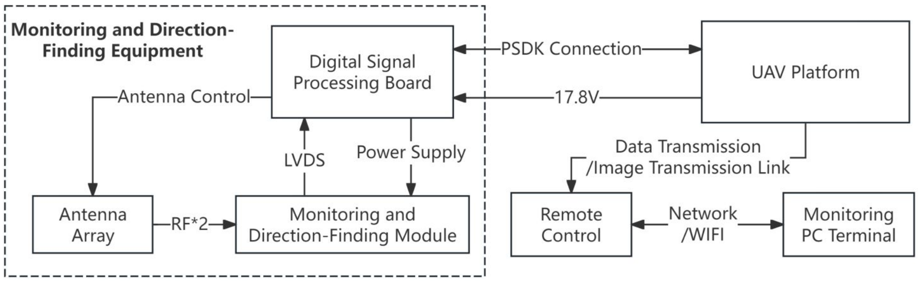

Fig. 1: Overall Structure of the UAV Interference Source Direction-Finding System

Fig. 2: Physical Image of UAV Flight Status

supports high-speed continuous shooting at 0.7 -second intervals, effectively avoiding the "jello effect". It also supports the connection of an RTK module to achieve centimeter-level high-precision positioning.

(2) Monitoring and Direction-Finding System

The monitoring and direction-finding system includes a receiver and a 5 -element antenna array. The structure of the aerial monitoring and direction-finding payload is shown in Figure 4. This system is composed of a 5 -element antenna array and a monitoring and direction-finding module, with a receiving frequency range of 100MHz – 6GHz.

Among them, SP2T and SP4T refer to Single-Pole Double-Throw and Single-Pole Four-Throw microwave switches, respectively. The SP2T is mainly responsible for the antenna selection function, choosing the corresponding antenna from A, B, C, D, and E to receive signals; the SP4T is mainly responsible for the signal path allocation function, distributing the selected signal to the corresponding signal processing channel.The microwave switches are controlled by signals output from the digital signal processing board. Specifically, the radio frequency (RF) channel RF1 can select array elements A and B as inputs, while the RF channel RF2 can select array elements B, C, D, and E as inputs. Therefore, there are 7 combinations of RF inputs, as shown in the truth table (Table 1). Here, vc1, vc2, and vc3 are the control voltage signals sent by the digital signal processing board: vc2 is responsible for controlling the SP2T switch, and vc1 and vc3 are responsible for controlling the SP4T switch. In addition, " 0 " represents a low level, and " 1 " represents a high level.By using these 7 antenna combinations, a phase difference matrix is obtained. Then, coherence analysis is performed based on the existing sample data, thereby achieving high-precision direction finding of the interference source.

Table 1: Truth Table for RF Input

vc 1	vc 2	vc 3	RF 1	RF 2
0	0	0	A	C
0	0	1	A	D
0	1	0	B	C
0	1	1	B	D
1	0	0	A	E
1	0	1	A	B
1	1	0	B	E

The AD9361 chip receives, amplifies, and frequency-converts the radio frequency (RF) analog signals filtered by the front-end switch network, and finally converts them into digital signals. These digital signals are output to the digital signal processing board via the LVDS interface for subsequent analysis.

The direction-finding antenna array used for collecting spatial electromagnetic signals adopts a five-element dual-hammerhead antenna array structure model, as shown in Figure 5. The positions of the antennas are uniformly distributed in terms of direction, and the directional gain range within the system's receiving frequency range is ±1.5dBi.

2.2 Monitoring and Direction-Finding Signal Acquisition and Processing Method

2.2.1 Direction-Finding Platform Data Link

The system operation block diagram is shown in Figure 6. Among them, the aerial part includes the

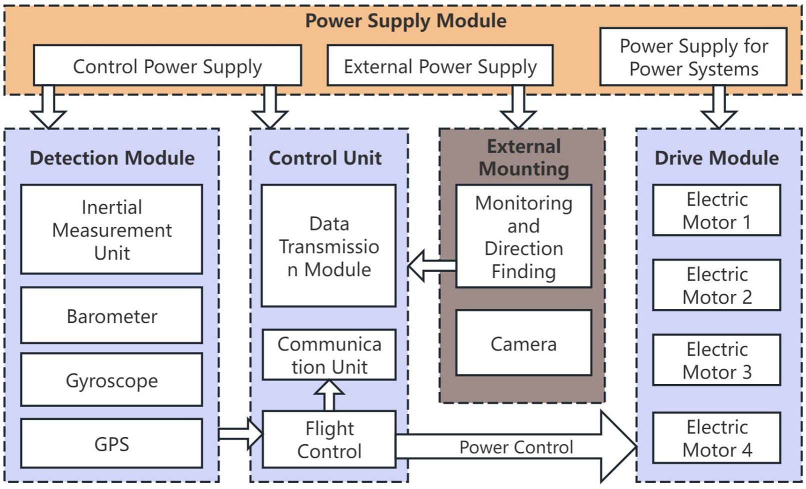

Fig. 3: UAV Platform Structure

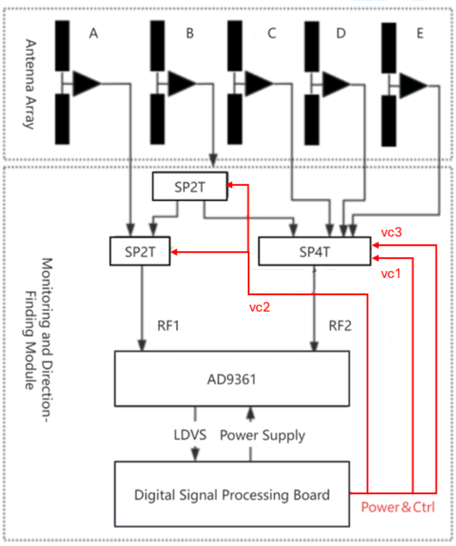

Fig. 4: System Structure of Monitoring and Direction-Finding Payload

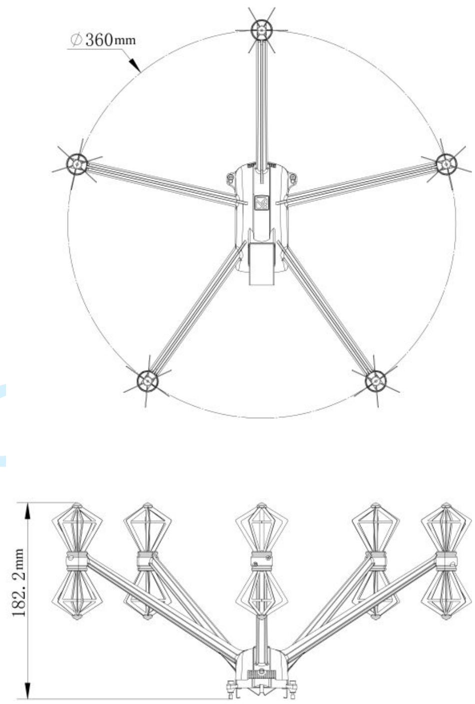

Fig. 5: Schematic Diagram of Antenna Array Mounting

UAV and the integrated monitoring and direction-finding module carried by the UAV; the ground station part includes the remote controller and the monitoring PC terminal. In the monitoring and direction-finding module, RF1 and RF2 are the output ports of the antenna array, and AD9361 is a software-defined RF transceiver chip. It supports a wide frequency range from 70 MHz to 6 GHz and provides a configurable digital interface, which simplifies integration with the processor.

In the data receiving process:

First, the signals received by the antenna array pass through a band-pass filter and an amplifier, and then the two channels of RF signals are input to the AD9361 chip. This chip adopts zero-IF (Intermediate Frequency) receiving technology, which converts the input high-frequency analog signals into zero-IF signals through IQ mixing [11].

Second, the signals are sampled and converted into digital signals by an ADC (Analog-to-Digital Converter), and then transmitted to the digital signal processing board via the LVDS (Low Voltage Differential Signaling) interface for coherent interference direction-finding and positioning, so as to determine the relative direction of the interference source.

Third, the digital signal processing board transmits data back to the UAV platform through the PSDK

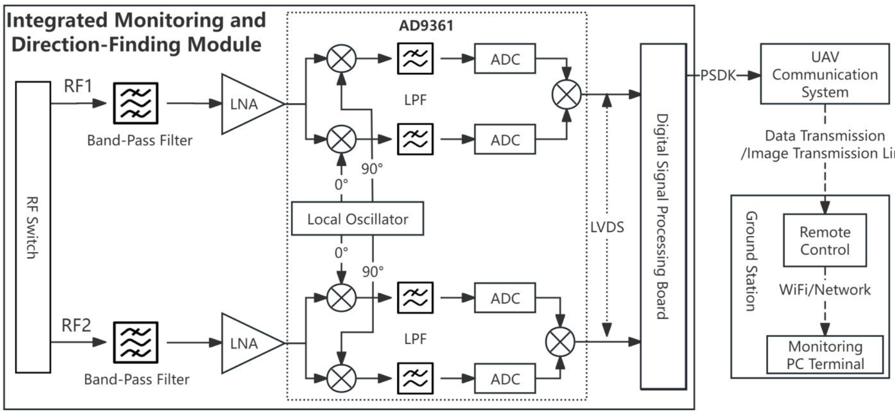

Fig. 6: Data Reception Link of the Direction-Finding Platform

(Payload Software Development Kit) interface for further analysis.

Finally, the ground station part consists of the remote controller of the UAV platform and the monitoring PC terminal. After the RF digital signals processed by the digital signal processing board are transmitted back to the UAV platform, they are sent back to the ground station through the data transmission/video transmission link for data storage and further processing. At the same time, the remote controller and the monitoring PC are connected via a network to view the UAV status in real time.

2.2.2 Principle of Coherent Interference Direction-Finding

The coherent interferometer direction-finding algorithm is widely used in military and civilian direction-finding system architectures due to its advantages, such as high direction-finding accuracy and adaptability to various antenna array structures [12]. Traditional interferometric direction-finding is based on the acquisition of the incident wave phase distribution by antenna array elements, and realizes direction-finding by measuring the phase difference between the voltages received by each antenna array element in the direction-finding antenna system. The direction-finding model of the one-dimensional single-baseline phase interferometer is shown in Figure 7.

When a plane wave with frequency f (wavelength $\lambda = c/f$, where c is the speed of light) arrives at two direction-finding antennas (Antenna 1 and Antenna 2) spaced by a distance L from a direction forming an included angle θ with the antenna boresight, the phase difference φ (in radians) between the signals received by the two antennas is

$$\varphi = \frac{2\pi L}{\lambda} \sin\theta \tag{1}$$

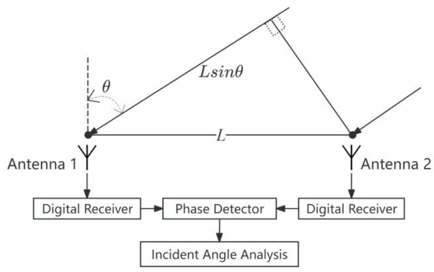

Fig. 7: Basic Principle of Single-Baseline Interferometer

After performing the angle transformation, the incident angle of the plane wave is calculated as shown in the formula (2).

$$\theta = \arcsin\left(\frac{\varphi\lambda}{2\pi\ \mathrm{L}}\right) \tag{2}$$

After obtaining the phase difference φ of the two signals through a phase detector, the incident angle of the plane wave can be calculated.

However, in practical applications, there is mutual coupling between antenna array elements, and the antenna bracket may cause distortion and deformation of the wavefront. Such situations often reduce the direction-finding accuracy [13]. Therefore, to improve the direction-finding accuracy, the system in this paper adopts a multi-baseline five-element antenna array for coherent interference direction-finding. Specifically, the incident direction is determined by comparing the similarity between the acquired incident wave phase distribution and the azimuth and incoming wave phase distribution of the existing original samples.

The direction-finding model is shown in Figure 8, where $\mathrm{A, B, C, D,}$ and E represent receiving array elements, which are uniformly distributed on a circle with radius R. It is assumed that a signal with frequency f is incident parallel to the antenna array elements, and α is the incident direction of the interference signal.

The switching of antenna pairs is automatically and sequentially completed by the digital signal processing board through control voltages (vc1, vc2, vc3). The switching frequency depends on the required signal processing gain and the tracking requirements for dynamic signals. Within one positioning measurement cycle, the system traverses the seven antenna combinations listed in Table 1 within the millisecond scale to collect phase difference data of all baselines. The whole process is automatic without manual intervention. After the UAV flies to the predetermined direction-finding point, the system automatically executes the above process and outputs the results. Path planning is mainly used to guide the UAV to different direction-finding points for subsequent intersection positioning.

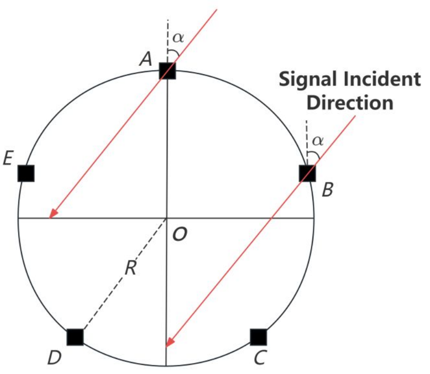

Fig. 8: Top-Down Simplified Model of a 5-Element Uniform Circular Array (Black Dots Represent Element Positions)

At this time, the receiver is connected to antenna elements A and B, and the phase difference ϕ_{BA} between antennas A and B can be obtained by reading the phase difference output by the phase detector. By changing the array elements connected to RF1 and RF2, the phase difference matrix can be derived:

$$\phi = [\phi_{\mathrm{BA}}, \phi_{\mathrm{CA}}, \phi_{\mathrm{DA}}, \phi_{\mathrm{EA}}, \phi_{\mathrm{CB}}, \phi_{\mathrm{DB}}, \phi_{\mathrm{EB}}] \quad (3)$$

Then, the coherence coefficient ρ between the phase difference matrix ϕ and the data sample $\phi_{(f,\alpha)}$ is calculated, as shown in Formula (4):

$$\rho = \frac{\phi \times \phi_{(f,\alpha)}}{\sqrt{\phi^2 \times \phi_{(f,\alpha)}^2}} \quad (4)$$

Finally, the sample data $\phi_{\max(\mathrm{f}_0,\alpha_0)}$ corresponding to the maximum coherence coefficient $\rho_{\max}$ is selected. The α_0 corresponding to the frequency f_0 of this sample data is the test result of the azimuth angle. Based on this, the incident direction of the plane wave is determined, and a direction-finding line is drawn, thereby providing a basis for interference source positioning.

2.2.3 Implementation of Intersection Positioning

As the direction parameter is one of the most reliable parameters of the target signal source, the direction-finding cross positioning method is the earliest developed, most studied, and most widely used passive positioning method [14]. This algorithm mainly uses the azimuth angle information of the target signal source measured at different geographical locations to obtain corresponding positioning direction-finding lines, and then determines the position of the target signal source through mathematical and geometric principles. Since the intersection positioning method requires direction-finding of the interference source at multiple locations, the high mobility of the UAV provides convenient advantages for intersection positioning. The intersection positioning process in this system is shown in Figure 9.

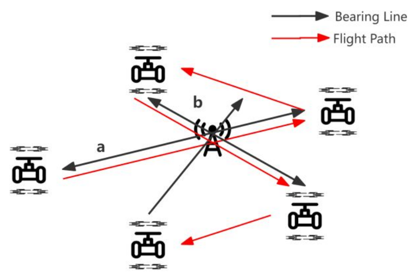

Fig. 9: Process and Principle of Intersection Positioning

In Figure 9, the red path represents the UAV's flight path, and the black paths represent the direction-finding lines. The process of UAV interference source positioning can be summarized as follows:

Step 1: Set the receiver to the target interference frequency and perform direction-finding on-site to obtain the interference source direction-finding line a;

Step 2: Fly in the direction of the direction-finding line while monitoring the change in field strength. Stop the UAV when the field strength changes from high to low, the UAV operator manually controls the UAV to hover and reacquire the direction-finding line of the interference source.

Step 3: Rotate the UAV by a certain angle, fly straight for a certain distance, hover, and conduct another test to obtain the interference source direction-finding line b.

Step 4: Repeat the above process to obtain multiple interference source direction-finding lines until they intersect at a single point, thereby achieving precise positioning of the interference source.

3. FIELD TEST VERIFICATION AND ERROR ANALYSIS

During the field experiment, a signal source was used to simulate the interference source to be locatedThe signal source consists of a programmable signal generator, Keysight N5172B, equipped with a dipole antenna. After on-site investigation and analysis, Nongke Village, Pixian District, Chengdu City, was selected as the experimental verification site, and its geographical location is shown in Figure 10.

After confirming that the power and network cables near the experimental site would not affect the test process and that the area is not a no-fly zone, an interference source was artificially placed at a concealedn location. Subsequently, the UAV platform was used to conduct the following analyses on the position of the interference source and the interference radiation within the area:

(1) Perform intersection positioning to determine the position of the interference source and verify the accuracy of interference source positioning;

(2) Test the radiation response of the interference source in the area at the interference frequency, generate an electromagnetic situation map, and determine the influence range of the interference source.

Fig. 10: Schematic Diagram of the Geographical Location of Nongke Village, Pidu District, Chengdu City

3.1 Intersection Positioning Test

To test the direction-finding accuracy of the UAV, the interference source was first placed at different orientations relative to the system. Subsequently, the test results were compared with the actual reference angles, and some of the obtained test results are shown in Table 2, where the 0° direction is defined as the heading of the UAV. A single-frequency continuous-wave (CW) signal is transmitted during the test. The test results are obtained by manually setting the signal source to transmit sequentially at different frequency points and performing direction-finding point by point, so as to evaluate the system performance at different frequencies.

Subsequently, the test data for all interference source directions were plotted into the error graph shown in Figure 11. Here, the horizontal axis represents the transmission frequency of the interference source, the vertical axis represents the relative error between the test results and the actual results, and the actual angular interval between the placed interference sources in the test was 45°.

From the above tests, it can be concluded that the direction-finding accuracy of the system is better than 5°, and this performance endows it with excellent interference source positioning capability. Furthermore, when the orientation of the interference source is unknown, the intersection positioning method is used to locate the position of the interference source. When multiple direction-finding lines stably intersect at the same point, the interference position can be obtained, realizing the single-station multi-point intersection positioning function. Figure 12 shows the test process and results of the position interference source. During the test of the 1401.1 MHz interference source, the UAV took off on-site, obtained the approximate direction of the interference source through testing, and then drew the interference source direction-finding line. The relative position of the UAV was changed multiple times to draw direction-finding lines, and the precise position of the interference source was obtained.

In this test, the actual longitude and latitude of the interference source were (E103.799798, N30.813690), and the measured longitude and latitude were (E103.799771, N30.813708), with a measurement error of approximately 4 meters.

3.2 Spatial Electromagnetic Situation Analysis and Testing

The main purpose of spatial electromagnetic situation map analysis is to check the influence range of the interference source. Therefore, in this test, the transmission

Table 2: Partial Results of Direction-Finding Accuracy Test

Direction of Interference Source	0°		45°		90°	
Frequency(MHz)	Direction Line/ °	Error/ °	Direction Line/ °	Error/ °	Direction Line/ °	Error/ °
1100.1	356.8	-3.2	44.8	-0.2	88.8	-1.2
1200.1	359.0	-1.0	44.7	-0.3	88.6	-1.4
1300.1	1.7	1.7	44.3	-0.7	88.5	-1.5
1400.1	359.8	-0.2	43.8	-1.2	88.0	-2.0
1500.1	0.3	0.3	45.0	0.0	88.9	-1.1
1600.1	358.2	-1.8	45.0	0.0	88.9	-1.1
1700.1	358.1	-1.9	42.7	-2.3	88.8	-1.2
1800.1	358.1	-1.9	41.9	-3.1	89.3	-0.7
1900.1	359.4	-0.6	41.2	-3.8	90.3	0.3
1999.1	359.8	-0.2	43.5	-1.5	88.7	-1.3
Average Error	-0.9		-1.3		-1.1	

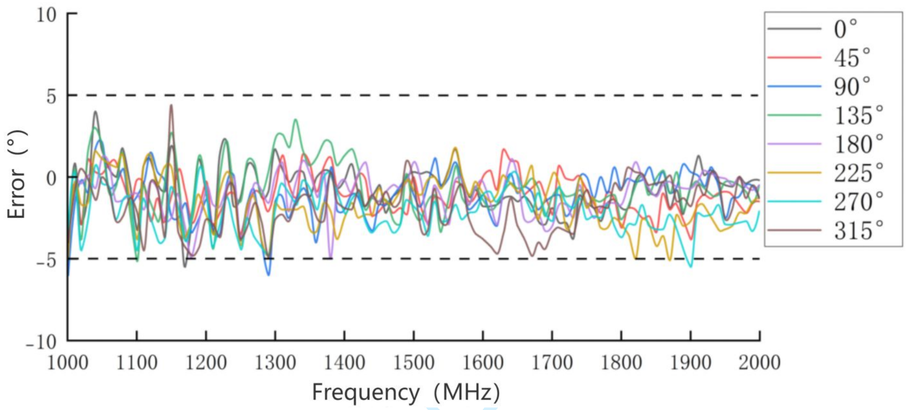

Fig. 11: Test Results of System Interference Source Direction-Finding Error

Fig. 12: Intersection Positioning Test and Results

frequency of the signal source was set to 1501.1 MHz and the transmission power to 1 W, which were used as the test objects for analysis. The test distance interval was 20 meters, the test altitude was 35 meters, and the radiation analysis covered an area of approximately 0.33 square kilometers (about 640 meters in length and 520 meters in width). The UAV's flight path and test results are shown in Figure 13. To accurately locate ground targets, the system adopts an annular progressive approximation flight strategy. The flight trajectory of this strategy is manifested as a set of concentric circles centered on the target. Starting from an initial distance, the UAV flies sequentially along circular flight paths with gradually decreasing radii. During each circular flight, the airborne radio frequency direction-finding system continuously scans the target signal and calculates the direction-finding angle. Through this periodic circular flight, the system can continuously collect direction-finding data from different directions, and gradually converge and accurately estimate the target position using triangulation positioning or filtering algorithms. Meanwhile, the stable control of flight altitude and speed ensures the continuity and reliability of data collection. This strategy effectively overcomes the uncertainty of single-point direction-finding and achieves continuous improvement of positioning accuracy with the flight process through path planning.

Point H in Figure 13 is both the UAV's take-off position and the location of the interference source. The closer the area is to the interference source, the higher the measured interference level. In the results of this test, the interference level in the central area reached 54.6 dBuV,

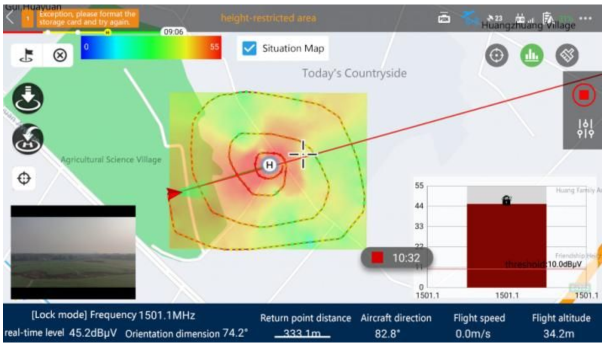

Fig. 13: Test Process of Electromagnetic Situation Map

and the minimum measured interference level was 34 dBuV. The electromagnetic situation map is drawn based on the exported raw data. During the drawing process, we adopt a spatial interpolation algorithm on the longitude, latitude, and field strength data collected at discrete points (actual UAV measurement points) to estimate the field strength values in the regions between measurement points, thus forming a continuous distribution view, as shown in Figure 14.

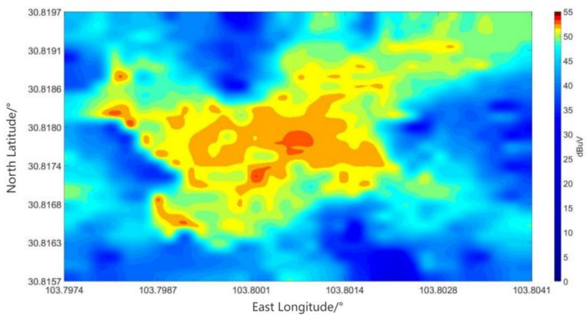

Fig. 14: Test Results of Electromagnetic Situation Map

Here, the horizontal axis represents longitude (range: E103.7974° to E103.8041°), and the vertical axis represents latitude (range: N30.8157° to N30.8197°). The radiation intensity of the interference source shows a trend of gradually decreasing from the central area to the surrounding areas. Due to the radiation pattern of the interference source's transmitting antenna and the influence of surrounding environmental factors, the attenuation trend of the interference signal varies in different directions.

3.3 Error Analysis

Possible sources of direction estimation and localization error in this experiment include: electromagnetic interference (EMI), systematic errors, signal and environmental errors, measurement and algorithmic errors, and operational errors.

(1)Electromagnetic interference (EMI):It is difficult to completely eliminate EMI on complex UAV platforms. Residual EMI may become one of the limiting factors for system sensitivity and introduce small errors in direction-finding for weak signals. In this field test, a relatively strong simulated interference source (1 W) was used, resulting in a high signal-to-noise ratio, so the influence of EMI was not dominant. However, when detecting weaker real-world interference, EMI is a factor that requires key consideration and calibration.

(2)Systematic errors:Amplitude-phase errors of the antenna array, deviations in antenna installation position, and disturbance of the antenna pattern by the UAV platform all have certain impacts on the test results. Precise calibration will be performed on the installation of various components of the antenna array and UAV platform in the future to reduce such errors.

(3)Signal and environmental errors:Multipath propagation (especially in complex terrain or near the ground), low signal-to-noise ratio (SNR), and co-channel or adjacent-channel interference are involved. In the follow-up flight path planning, direction-finding points at multiple different heights and angles will be selected as far as possible, and algorithms will be used to mitigate single-point multipath errors. When detecting weak interference sources, the signal-to-noise ratio (SNR) can be improved by increasing the antenna gain, optimizing the performance of the low-noise amplifier (LNA) in the receiver front end, or extending the signal integration time at each direction-finding point, thereby reducing the random phase errors caused by noise.

(4)Measurement and algorithmic errors:Phase measurement accuracy is limited by ADC and local oscillator phase noise, and the performance of the coherent interferometer algorithm degrades under low signal-to-noise ratio or in the presence of coherent sources. In future work, the azimuth sampling density will be increased and the calculation method of coherence coefficients will be optimized to reduce the influence of such errors.

(5)Operational errors:Attitude stability during UAV hovering, wind effects, and other factors.In the future, higher-precision GPS will be installed on the UAV, and automated flight algorithms will be designed to reduce delays and errors caused by manual judgment.

4. SUMMARY

This paper introduces a drone-based interference source localization and electromagnetic situation analysis system, aiming to solve the challenge of locating low-power interference sources that affect radio astronomical observations. The system adopts zero-IF (Intermediate Frequency) reception technology and coherent interferometry, enabling monitoring across the 1.1GHz – 2GHz frequency band and accurate localization of interference sources. Due to the design bandwidth of the AD9361 chip and the antenna array, the system theoretically supports real-time monitoring within the 100MHz – 6GHz frequency band. After subsequent algorithm optimization and error reduction, we will conduct tests at lower and higher frequency bands to achieve wideband real-time monitoring from 100 MHz to 6 GHz. Leveraging the flexibility and mobility of the drone platform, the system can quickly locate interference sources in complex terrains and generate electromagnetic situation maps to determine the interference coverage.

Field tests demonstrate that the system achieves an interference source localization accuracy better than 5°. Beyond precise localization, it can also measure the radiation of interference sources to plot electromagnetic situation maps. This provides robust data support for the identification and localization of interference sources in radio astronomy operations, as well as the planning and management of radio protection zones.

ACKNOWLEDGEMENTS

This work was supported by the following funds: the Special Project for Building a Science and Technology Innovation Center Facing South and Southeast Asia Yunnan Provincial International Joint Innovation Platform: "Yunnan Provincial China-Malaysia International Joint Laboratory of Advanced Radio Astronomy Technology at HF-VHF Bands" (Grant No. 202303AP140003); Advanced Array Technology Research and Development for Space Electromagnetic Sensing on the Technology "Compact Team" Talent Project,The Technology "Compact Team" Talent Project of Urumqi "Hongshan Science Innovation Talent" Cluster Program (Grant No. B241018006); the Cultivation Project of Joint Fund for Astronomy under the National Natural Science Foundation of China (Grant No. U2031133); the SKA Special Project of the Ministry of Science and Technology of the People's Republic of China (Grant No. 2020SKA0110202); the International Partnership Program of the Bureau of International Cooperation, Chinese Academy of Sciences: "Belt and Road" Cooperation (Grant No. 114A11KYSB20200001); the Kunming Municipal Foreign (International) Cooperation Base Project: "Joint R&D Cooperation Base for Advanced Radio Astronomy Technology between Yunnan Observatories, Chinese Academy of Sciences and University of Malaya" (Grant No. GHJD-2021022); the Key Special Project "Intergovernmental International Science and Technology Innovation Cooperation" under the National Key R&D Program of the Ministry of Science and Technology of the People's Republic of China: "China-Malaysia Cooperative Research on Space Remote Sensing and Radio Astronomy Observation of Space Weather at Mid-Low Latitudes" (Grant No. 2022YFE0140000); and the SKA Special Project of the Ministry of Science and Technology of the People's Republic of China - High-Precision Calibration Method for Low-Frequency Radio Interferometric Arrays (Grant No. 2020SKA0110300). Gratitude is expressed to Yunnan Observatories, Chinese Academy of Sciences for its support.

AI DISCLOSURE STATEMENT

During the preparation process of this work, we used the Grammarly tool to assist in English grammar checking and text polishing.

AUTHOR CONTRIBUTIONS

Hongrui Zhang participated in the review and editing of the manuscript, drafted the original version, and provided the research ideas. Liang Dong and Qiang Xi were responsible for hardware development and assisted in manuscript writing. Lesheng He took charge of the construction of the hardware platform. Shengyang Li and Bin Tian were responsible for providing the interference sources required for field tests. Ning Zhang was in charge of collating the test data. All authors have read and approved the final manuscript.

REFERENCES

[1] Zhang, H. Y. 2017. Progress in radio astronomical frequency protection in China. *Progress in Astronomy*, 35(04), 473–480.

[2] Zhao, Q. H., Li, J. B., & Zhang, T. 2020. Research on ranging-based localization algorithm in radio interference. *Astronomical Research & Technology*, 17(4), 446–453.

[3] Zhang, H. Y., Hu, H. L., Wang, Y., et al. 2022. Intelligent monitoring technology for radio interference of FAST. *Journal of Tsinghua University (Science and Technology)*, 62(11), 1780–1788.

[4] Zhu, K. H., Dong, L., & Li, J. F. 2024. Localization of high-elevation satellite interference signals based on joint time-frequency difference analysis. *Chinese Journal of Radio Science*, 39(4), 631–639+657.

[5] Li, J. 2021, Master's thesis, Anhui Jianzhu University, Anhui, (in Chinese)

[6] Memarian, Z., & Majidi, M. 2022. Multiple signals direction finding of IoT devices through improved correlative interferometer using directional elements. In proceedings of 2022 Sixth International Conference on Smart Cities.Mashhad, Iran

[7] Han, J., & Gao, J. 2022. Optimal estimation of direction finding for multi-baseline interferometer. *Electronic Information Warfare Technology*, 37(02), 38–43.

[8] Liu, D. R., Miao, S., Dong, L., et al. 2022. Test and research on direction of arrival of radio interference sources based on four-antenna array. *Astronomical Research & Technology*, 19(06), 552–558.

[9] Geng, L. H., Su, C., Du, J., et al. 2023. Solar Radio Observations and Simulations of Occultation Effects. *Astronomical Research Technology — Journal of National Astronomical*, 20(01), 15–23.

[10] Xiao, J. 2022. Research on Low-Altitude Electromagnetic Environment Monitoring and Electromagnetic Situation Visualization Based on UAV. *Civil Aviation Flight University of China*, .

[11] Devices, A. 2024, AD9361 RF Agile Transceiver Data Sheet (Rev. G), Technical Data Sheet, ,

[12] Han, G., Wang, B., & Wang, D. L. 2010. Research and implementation of coherent interferometer algorithm based on FPGA. *Application of Electronic Technique*, 36(07), 76–80.

[13] Li, J., Gao, H. T., & Zheng, X. 2005. Mutual coupling and near-field calibration of phased array antennas. *Acta Electronica Sinica*, (01), 119–122.

[14] Ma, R. 2019, Master's thesis, Huazhong University of Science and Technology, (in Chinese)

Dear Editor and Reviewers,

We sincerely thank you for taking the time to review our paper *Localization and Radiation Analysis of Interference Sources Based on UAV Platform* and for giving us the opportunity to revise the manuscript. We have carefully considered your valuable comments and suggestions, and have made thorough revisions and reorganizations to address them.All revisions have been highlighted in yellow in the text.

Reviewer 1

Comment 1：

In line 89, the paper introduces some application scopes of UAV technology in agriculture, logistics, emergency rescue. However, as an astronomical paper, cite more papers related to astronomical applications will be much better. For example, use UAV to measure the beam pattern of radio telescopes and use UAV photogrammetry to measure the surface accuracy of radio telescope and so on. In addition, be careful of Ref [10] (Guo, W. J. 2024). This paper seems to be of low quality. There is no substantial content, no reference, and even no conclusion. It’s better to remove this reference.

Response 1：

Thank you very much for your valuable suggestion. Following your advice, I have removed the reference cited in line 89 and replaced it with a reference that is more relevant to the topic of the article.

Comment 2：

Many nomenclatures are inconsistent. For example, in Fig. 3, it’s “Control Unit”, but in line 182, it’s “control module”. In Fig. 3, it’s “Power Supply Module”, but in line 181, it’s power module. In line 150, it’s “monitoring and direction-finding devices”, but in Fig. 1, it’s “Monitoring and Direction-Finding Equipment”. In line 183, it’s “UAV direction-finding system”, but in Fig. 3 caption, it’s “UAV Platform”. In line 190, it’s “external payload”, but in Fig. 3. it’s “External Mounting”. There are many more inconsistent nomenclatures. Please check through the whole paper and use consistent nomenclatures. Otherwise, the readers will get puzzled if these inconsistent nomenclatures are the same part or different parts.

Response 2：

Thank you very much for pointing out my mistake. According to your suggestion, I have revised all the naming conventions to be consistent with Figure 3.

Comment 3：

In Section 2.1, it's better to properly clarify which parts are already provided by the UAV (i.e. DJI Mavic 3E) and which parts are made by this work. It seems that only the external mounting/payload is made by this work. If so, the data transmission socket, or protocol or cables and so on between the external mounting/payload and the data transmission module should be introduced. So is the power socket design between the external mounting/payload and the external power supply.

Response 3：

Thank you very much for your valuable suggestion. Following your advice, I have clearly indicated at line 185 the components provided by DJI Mavic 3E and those developed by ourselves.

Comment 4：

In line 241, the vc and SP2T connection is not well described. It looks like vc2 is responsible for controlling the two SP2T switches simultaneously? If so, in Fig. 4, the 3 red lines should be modified. The two red lines to SP2T should be combined into one line with two arrows split at last and the red line to SP4T should be separated from the line to SP2T. In addition, there should be two red lines to SP4T. Also, draw labels vc1, vc2 and vc3 for these three red lines.

Response 4：

Thank you very much for pointing out my error. According to your suggestion, I have revised the red wiring part in Figure 4 and labeled vc1, vc2, and vc3.

Comment 5：

In line 351, how frequently to switch the antenna pairs? How long does it take to do one measurement for one baseline and all baselines? Is the whole process manually controlled or automatically done once path planning is made?

Response 5：

Thank you very much for your valuable suggestion. According to your advice, the switching of antenna pairs is automatically and sequentially completed by the digital signal processing board through the control voltages (VC1, VC2, VC3). The switching frequency depends on the required signal processing gain and the tracking demand for dynamic signals. In one positioning measurement cycle, the system quickly traverses the seven antenna combinations listed in Table 1 (within the millisecond order) to collect the phase difference data of all baselines. The entire process of "data acquisition – phase difference calculation – coherence analysis – azimuth output" is automated without manual intervention. After the UAV flies to the predetermined direction-finding point, the system automatically executes the above process and outputs the results. I have added the corresponding explanation to Line 361.

Comment 6：

In line 384, what do you mean to “Calibrate the interference frequency”?

Response 6：

The meaning of "calibrate the interference frequency" here is as follows: before starting on-site direction-finding and localization, the operator needs to use the spectrum monitoring function of the system to identify and lock the frequency of the specific interference signal to be detected. This is a standard operating procedure under the premise that the interference frequency is known but its bearing or position is unknown. Its purpose is to tune the receiver to the target frequency, ensuring that subsequent direction-finding and field-strength measurements are performed on this specific interference signal.

We have revised "Calibrate the interference frequency" to "Set the receiver to the target interference frequency" to avoid ambiguity.

Comment 7:

In Sec. 3, the signal source used to simulate the interference source is not described in detail. Add more description on its characteristics and composition, like the antenna type, directivity, single frequency or wide band and so on. This information would help to understand the sources of the errors in Figure 11. How is the measurement done for the continuous frequency range in Fig. 11? Do you measure the frequency points one by one or your signal source is wide band so can measure the whole frequency range in just one measurement? It would be better if the interference source is located several kilometers away from the UAV system. This would help to evaluate the sensitivity of the UAV system. And it’s more practical for real-world scenario as in radio astronomy, the interference sources are usually very far from the observatory.

Response 7:

Thank you very much for your valuable suggestion. According to your advice, we have added a description of the signal source of the simulated interference source at Line 424. Furthermore, we plan to conduct tests over several kilometers in future research, to more realistically evaluate the sensitivity and applicability of the system in the actual electromagnetic environment of radio observatories.

Comment 8:

As Table 2 and Fig. 11 show, most of the errors are negative and the average errors are about -1.1 degree. This seems to be a systematic error? As line 434 shows, the angular interval of the interference source is 45 degrees. How is the accuracy of this value? Is it a possible source of error for the systematic error? If the source of the systematic error is found and removed, the error can be further suppressed from 5 degrees to 4 degrees. In addition, how do you define the 0-degree direction of the interference source? Is it the head direction of the UAV, or the geographical north, or randomly chosen? Since the UAV is not rotational symmetric but bilateral symmetric, it would be better to define 0-degree to be the head direction of UAV. Using this definition, I wonder if similar error curves occur in Fig. 11 for bilateral symmetric directions like 45 deg and 315 deg, 90 deg and 180 deg and so on.

Response 8:

We highly appreciate the reviewer's insightful observation. This is indeed an important point for systematic error analysis. The average deviation of approximately -1.1° you pointed out clearly indicates the existence of a systematic error.

The total station used to measure the "actual reference angle" in the experiment also has its own error, but its accuracy (typically better than 0.5°) is higher than the systematic error we observed. Therefore, the reference angle error is not the dominant source of systematic error.

In this experiment, the 0° direction is defined as the heading of the UAV (i.e., its forward direction). This is a relative coordinate system that simplifies flight control. We have clarified this definition at Line 449 in the revised manuscript.

Finally, we have added a discussion on error analysis in Section 3.3.

Comment 9:

How do you make the 2D map of Fig. 14? Line 466 says the test interval was 20 meters.

However, it looks like the map in Fig. 14 has a high resolution possibly in several meters. From my understanding, you cannot obtain the signal strength of one place unless the UAV does measurement at that point. Therefore, using 20-meter test interval, how do you get a radiation distribution in precision of meters? Did you do some interpolation or using some radiation models?

Response 9:

Your understanding is completely correct. Based on discrete measurements at 20-meter intervals, data interpolation is necessary to generate the continuous, high-resolution color cloud map shown in Figure 14. In the revised manuscript, we will clearly state that when generating the electromagnetic situation map, we applied a spatial interpolation algorithm to the latitude, longitude, and field strength data collected at the discrete points (actual UAV measurement points) to estimate the field strength values in the regions between measurement points, thereby forming a continuous distribution view. We have briefly mentioned the plotting method at Line 527 in the manuscript.

Comment 10:

In line 515, the paper claims an application for frequency range from 100MHz to 6GHz, but this work only tested between 1.1GHz to 2GHz. The statement should be modified. As in low frequency range below 1GHz, the reflection effect of the UAV platform is probably getting much stronger, the beam pattern of the emitter antennas can change significantly, so the locating accuracy is decreased. Doing more tests covering frequency below 500MHz and also above 5GHz will benefit greatly.

Response 10:

We fully accept your comment. The current claim in the paper that the system supports 100 MHz – 6 GHz is based on the hardware capability (the design bandwidth of the AD9361 chip and the antenna array), whereas the experimental verification only covers the 1.1 – 2.1 GHz frequency band. In the revised manuscript, we have adjusted the relevant statement at Line 601, clearly indicating that in this experiment, we validated the system performance within the 1.1 – 2.1 GHz band, with a positioning accuracy better than 5° . Tests on lower and higher frequency bands will be included in our future work.

Comment 11:

What is the EMI situation of the UAV platform and the Monitoring and Direction-Finding Payload? Is the EMI on the whole system well controlled? Does the EMI introduce errors in the field test result?

Response 11:

Thank you very much for your valuable suggestion. We acknowledge that it is difficult to completely eliminate EMI on a complex UAV platform. Residual EMI may become one of the limiting factors for the system sensitivity and could introduce minor errors in direction-finding for weak signals. In this field test, the impact of EMI was not dominant because a relatively strong simulated interference source (1 W) was used, resulting in a high signal-to-noise ratio. However, EMI is an important factor that needs to be carefully considered and calibrated when detecting weaker real-world interference. We have added a discussion on EMI in the error analysis of Section 3.3.

Comment 12:

Ref [1] and Ref [9] are repeated. In latex, the double opening quote should be `` (two back quotes located below ~ button).

Response 12:

Thank you very much for pointing out my error. According to your suggestion, we have removed Reference 9.

Reviewer 2

Comment 1:

In the step of cross-localizing interference sources, direction-finding lines are re-acquired when the measured field strength decreases. It is necessary to clarify whether this step relies on manual qualitative judgment of the field strength， or is an automatic operation triggered by a preset threshold in the system.

Response 1:

In the current system, this step relies on the operator’s real-time monitoring and judgment. The operator observes the trend of the Received Signal Strength Indicator (RSSI) on the monitoring software. When the RSSI changes from increasing to decreasing (indicating that the UAV may have flown past the closest point to the interference source), the operator manually controls the UAV to hover and perform a second direction-finding. In the revised manuscript, we have clarified at Line 409 that this is currently a human-machine interactive step. Meanwhile, we will point out in the discussion section that implementing an automatic threshold trigger is a direction for future system upgrades, which can further improve the automation and efficiency of the localization process.

Comment 2:

Can the proposed method simultaneously realize direction-finding and localization for two or more interference sources, regardless of whether they have the same or different frequencies?

Response 2:

The core direction-finding algorithm (coherent interferometer) proposed in this paper is generally used for direction-of-arrival estimation of a single signal source. For multiple interference sources with different frequencies, the system can separate them in the frequency domain through frequency scanning or wideband processing, and then theoretically perform direction-finding and subsequent cross-location for each frequency individually. However, for multiple coherent or incoherent interference sources at the same frequency, the current system based on the conventional coherent interferometer is difficult to directly distinguish and locate simultaneously without adopting more advanced array signal processing algorithms. This is indeed a limitation of the current system and an important direction for future research.

Comment 3:

In the experiments on direction-finding and localization of interference sources in partial frequency bands, the error is less than 5 degrees angle. It is required to confirm whether the system can be reliably applied within the frequency range of 100 MHz – 6 GHz. Additionally, please elaborate on the possible factors that may lead to direction-finding and localization errors.

Response 3：

Thank you very much for your valuable suggestion. We have revised the manuscript to clearly state that the direction-finding accuracy better than 5° was verified only in the 1.1 – 2.1 GHz band in this experiment. The system hardware supports a wider frequency band, but reliable operation across the full band (100 MHz – 6 GHz), especially maintaining consistent accuracy, requires more comprehensive tests and possibly band-dependent calibration.